

ARTICLES

An Interesting Isotope Effect in the Raman Excitation Profile for HI

N. Chakrabarti[†] and N. Sathyamurthy^{*‡}

Department of Chemistry, Indian Institute of Technology, Kanpur 208 016 India

Received: May 4, 1998

It is shown that the Raman excitation profile for the fundamental Stokes transition of DI in the vicinity of its electronic transition to the nearby dissociative states exhibits a larger deenhancement than that for HI, as a result of larger interference between the resonance Raman amplitudes for the four closely lying excited (dissociative) electronic states.

1. Introduction

Resonance Raman spectra provide valuable insight into the short time dynamics of excited states of molecules,^{1,2} much more than the corresponding photoabsorption spectra do. The variation of resonance Raman intensity with the excitation wavelength (λ), called the Raman excitation profile (REP), is nearly identical to the absorption spectrum, if the resonance Raman scattering involves only one excited electronic state. If there are more than one excited electronic states lying close to each other and they are accessible to the molecule under the influence of the exciting radiation, there is likely to be interference between different parts of the wave function evolving on the different excited potential energy curves and, hence, between Raman amplitudes arising from different channels (see below). The extent of interference would, understandably, depend upon the number and nature of the excited electronic states, energy spacing, and nonadiabatic coupling between them and their transition dipole moments. In contrast to the overall enhancement in the Raman signal, one observes, when there is an excited state mediation, there could be a drop in the enhanced intensity for certain λ 's, resulting from the interference. This is referred to as antiresonance or resonance deenhancement in the literature. The location and the extent of the dip in the REP can be quite

revealing of the nature and magnitude of the interference. Some of the examples of resonance Raman deenhancement reported so far can be found in refs 3–5 and references therein.

In an earlier publication⁵ we had reported the computed REP for HI corresponding to the fundamental Stokes line originating from the ground electronic state ($X^1\Sigma_0$) and mediated by the first four excited electronic states ($1 = ^3\Pi_1$, $2 = ^1\Pi_1$, $3 = ^3\Sigma_1$, and $4 = ^3\Pi_0$) using time-dependent quantum mechanical (TDQM) wave packet approach.⁶ The possibility of observing resonance Raman deenhancement arising from the interference between Raman amplitudes for the different close lying excited electronic states was pointed out. It was further shown that the entire time evolution on the excited states was over within about 10 fs and that overtones exhibited a larger deenhancement effect.

The longer the time evolution on the excited states, the greater is the likely interference. Substitution of H by D in HI results in a significant difference in the initial wave function and also in considerable slowing down of the dynamics. The reduced mass of DI is 1.98 times that of HI. While the ground electronic state of DI supports 30 vibrational states and the fundamental vibrational period is ~ 21 fs, the number of bound states is 21 for HI, and the period of oscillation for the fundamental vibration is ~ 15 fs. In addition, the potential curves, nonadiabatic couplings, and the transition dipole moments for the first four excited states of DI differ slightly from those of HI. For quick reference, we list the values of the transition dipole moments

[†] Present address: Département de Chimie, Université de Montréal, C.P. 6128, succ. Centre-Ville, Montréal H3C 3J7, Canada.

[‡] Honorary Professor, S. N. Bose National Center for Basic Sciences, Calcutta, India.

TABLE 1: Transition Dipole Moments for HI and DI⁷

molecule	³ Π ₁	¹ Π ₁	³ Σ ₁	³ Π ₀
HI	0.007 830 4	0.019 287	0.009 983	0.011 451
DI	0.007 871	0.017 91	0.010 364	0.011 26

TABLE 2: Off-Diagonal Potential Energy Elements in the Hamiltonian Matrix for HI and DI⁷

HI	³ Π ₁	¹ Π ₁	³ Σ ₁
³ Π ₁		0.001 959	0.001 909
¹ Π ₁	0.001 959		0.001 620
DI	³ Π ₁	¹ Π ₁	³ Σ ₁
³ Π ₁		0.002 549	0.002 018
¹ Π ₁	0.002 549		0.001 705

in Table 1 and the coupling elements in Table 2 for the first four excited electronic states of HI and DI.⁷ For DI, the transition dipole moment for excited state 2 (¹Π₁), for example, is ~10% lower than that for HI. Off-diagonal potential matrix element V_{12} (between states ³Π₁ and ¹Π₁) for DI is ~25% higher than that of HI. Therefore, we expect that all these factors put together along with slower nuclear motion in DI (compared to HI) will contribute to a larger degree of interference and hence larger deenhancement in DI.

The basic methodology in computing REPs is described in section 2 and the results for DI are presented and discussed in section 3. Summary and conclusions follow in section 4.

2. Methodology

The most important quantity to be determined in the TDQM methodology is the time correlation function $C(t)$ ⁸ of the wave packet. This is essentially of two types. One is the autocorrelation function,

$$C_{ii}(t) = \langle \phi_i(0) | \phi_i(t) \rangle \quad (1)$$

where $\phi_i(0) = \mu_{e-g} \psi_i(0)$, with $\psi_i(0)$ being the wave function for the initial vibrational state i in the ground electronic state and $\phi_i(t)$ representing the corresponding promoted state wave function evolving with time under the influence of the excited state Hamiltonian. μ_{e-g} is the transition dipole moment. Fourier transform of the autocorrelation function yields the absorption cross section^{9–11}

$$\sigma_A(\omega_I) = \frac{2\pi\omega_I}{3\hbar c} \int_{-\infty}^{\infty} C_{ii}(t) e^{i(\omega_I + \omega)t} dt \quad (2)$$

corresponding to molecules with initial vibrational frequency ω_i subjected to incident photons of frequency ω_I . In case the time evolved wave function in the excited state is correlated to some other ($f \neq i$) vibrational state in the ground electronic state, we compute the cross correlation function:^{12,13}

$$C_{fi}(t) = \langle \phi_f(0) | \phi_i(t) \rangle \quad (3)$$

where $\phi_f(0) = \mu_{e-g} \psi_f(0)$ is the wave function corresponding to the vibrational state f in the ground electronic state. The time domain complex quantity $C_{fi}(t)$ is mapped on to another complex quantity called the Raman amplitude ($\alpha_{fi}(\omega_I)$) in the energy domain via the (half) Fourier transform relationship:^{12,13}

$$\alpha_{fi}(\omega_I) = \frac{i}{\hbar} \int_0^{\infty} C_{fi}(t) e^{i(\omega_I + \omega)t} dt \quad (4)$$

The squared modulus of Raman amplitude yields the observable called Raman intensity,

$$I_{fi}(\omega_I) = \omega_I \omega_S^3 |\alpha_{fi}(\omega_I)|^2 \quad (5)$$

where ω_S is the frequency of the scattered radiation.

All these relationships described so far are for a system with a single excited state. For a system involving more than one excited electronic state, we need to compute quantities such as $C_{ii}^l(t)$ and $C_{fi}^l(t)$ for each channel (or excited electronic state) l and the corresponding partial absorption cross sections $\sigma_A^l(\omega_I)$ and channel specific Raman amplitudes $\alpha_{fi}^l(\omega_I)$. Thus

$$\sigma_A^l(\omega_I) = \frac{2\pi\omega_I}{3\hbar c} \int_{-\infty}^{\infty} C_{ii}^l(t) e^{i(\omega_I + \omega)t} dt \quad (6)$$

$$\alpha_{fi}^l(\omega_I) = \frac{i}{\hbar} \int_0^{\infty} C_{fi}^l(t) e^{i(\omega_I + \omega)t} dt \quad (7)$$

The total absorption cross section is defined as

$$\sigma_A(\omega_I) = \sum_l \sigma_A^l(\omega_I) \quad (8)$$

and the total Raman amplitude

$$\alpha_{fi}(\omega_I) = \sum_l \alpha_{fi}^l(\omega_I) \quad (9)$$

The Raman intensity for the system is proportional to the squared modulus of total Raman amplitude:

$$I_{fi}(\omega_I) = \omega_I \omega_S^3 |\alpha_{fi}(\omega_I)|^2 \quad (10)$$

We have considered DI to be initially in its ground vibrational state ($i = 0$) of its ground electronic state. The time evolution of the excited state wave function is governed by the coupled differential equation:⁵

$$i\hbar \frac{\partial}{\partial t} \begin{pmatrix} \phi^1 \\ \phi^2 \\ \phi^3 \\ \phi^4 \end{pmatrix} = \begin{pmatrix} H_{11} & V_{12} & V_{13} & 0 \\ V_{21} & H_{22} & V_{23} & 0 \\ V_{31} & V_{32} & H_{33} & 0 \\ 0 & 0 & 0 & H_{44} \end{pmatrix} \begin{pmatrix} \phi^1 \\ \phi^2 \\ \phi^3 \\ \phi^4 \end{pmatrix} \quad (11)$$

where the symbols have their usual meaning. Fast Fourier transform (FFT) algorithm was used for spatial evolution and second order differencing (SOD) scheme for temporal evolution of the wave packet.⁶

The coordinate space consisting of the D–I bond distance was discretized into 512 equispaced grid points in the range 1.0–21.44 a_0 and time evolution was carried out for 16 384 steps of 2.41889×10^{-3} fs each (for a total of 39.63 fs).

3. Results and Discussion

For the sake of clarity and completeness, we show the potential energy curves for DI in Figure 1a. The curves for HI are practically superimposable on the curves for DI and hence are not shown here. The differences in the off-diagonal elements for HI and DI, however, are noticeable, as can be seen from Figure 1b.

Population variation with time in the excited states is shown in Figure 2a for DI. The initial population in each state reflects the magnitude of the corresponding transition dipole moment squared. Because the excited state $l = 4$ is not coupled to any other state, the population in that state remains constant with time. The exchange of population between states 1, 2, and 3 reflects the strength of coupling between them. For comparison, the results for HI are included in Figure 2b. We see that

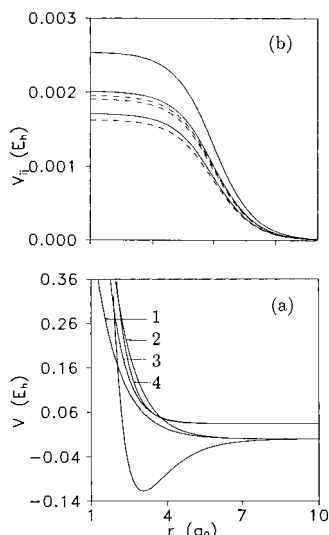


Figure 1. (a) Potential energy curves for DI, (b) off-diagonal elements for DI (solid lines) and HI (dashed lines).⁷

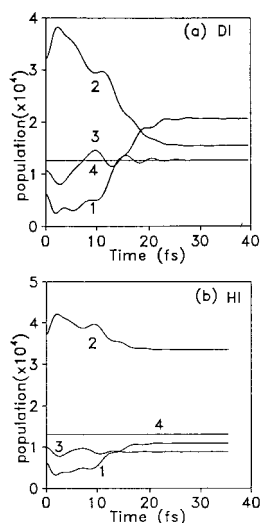


Figure 2. Population variation with time on the four excited states of (a) DI and (b) HI.

interelectronic coupling is clearly greater and it lasts longer for DI than for HI.

The cumulative value of the autocorrelation function is plotted in Figure 3a for DI as well as for HI. The decay is a bit slower for the former than for the latter as expected. The difference in the initial values of C_{00} for the two systems reflects the difference in transition dipole moment values for the four excited states in DI and HI:

$$C_{00}(0) = \sum_{l=1}^4 |\mu_l|^2 \quad (12)$$

We plot in Figure 3b the total absorption cross section for DI and HI. They have qualitatively the same shape, although σ_A for DI has a slightly higher peak value than that for HI. This might be indicative of a larger “cross-term” interference³ in DI than HI.

The cross correlation function for the fundamental Stokes Raman transition ($i = 0, f = 1$) obtained from the TDQM calculations is plotted in Figure 3c for DI along with the results for HI. The higher peak value for HI is, once again, reflective of the larger value of μ for HI than for DI. The Raman

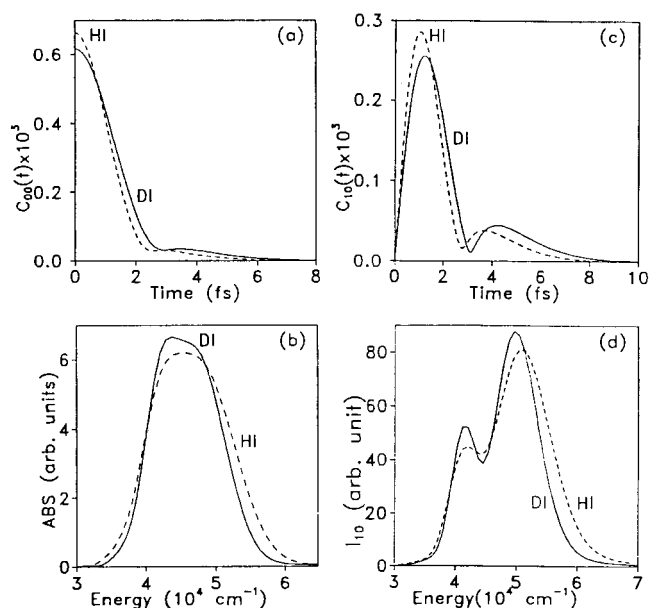


Figure 3. The cumulative autocorrelation function for HI (dashed line) and DI (solid line), (b) the total absorption cross section for HI (dashed line) and DI (solid line), (c) the cumulative cross correlation function for HI (dashed line) and DI (solid line), (d) the total continuum Raman excitation profile for the fundamental Stokes transition in HI (dashed line) and DI (solid line).

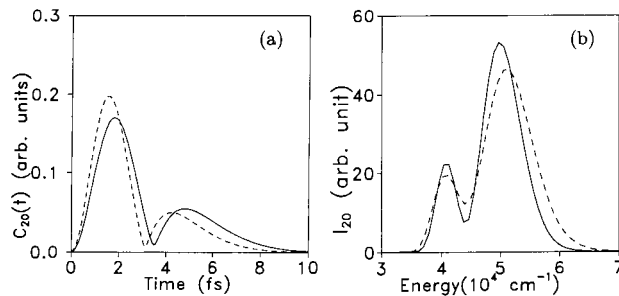


Figure 4. (a) The cumulative cross correlation function and (b) the Raman excitation profile for HI (dashed line) and DI (solid line) for the first vibrational overtone ($i = 0, f = 2$) transition.

excitation profiles obtained for the two systems are plotted in Figure 2d. Although they are qualitatively similar, the resonance deenhancement is clearly more pronounced for DI than for HI.

That the effect becomes even more pronounced for the overtones than for the fundamental transition becomes evident when we examine the cross correlation functions and the REPs for the first overtone for the two systems, shown in Figure 4. The dominant factors which govern the interference effects (the width and depth of the deenhancement) are the values of the transition dipole moments, nonadiabatic coupling elements, energy proximity of the electronic states, their slopes, and the mass of the system undergoing dynamical motion. As parametrized by Levy and Shapiro,⁷ all the interelectronic coupling elements are larger for DI than for HI and the sum of the squared transition dipole moments are smaller for DI than for HI. The reduced mass of DI is 1.98 times that for HI. Hence, DI moves more slowly along the potential energy curves and the interelectronic coupling is experienced by DI for a longer period of time. The composite effect of all these factors is a larger interference between the Raman amplitudes for the different channels and hence a larger deenhancement in DI than in HI.

4. Summary and Conclusion

We have found an interesting isotope effect in the Raman excitation profile for a dissociative system like HI(DI). To the

best of our knowledge, such an effect has not been reported till this date. It is experimentally verifiable and is likely to manifest in similar diatomic systems or for vibrational modes of polyatomic systems for which isotopic substitution results in a substantial change in the reduced/effective mass and other factors mentioned above. We hope that the present study would provide enough incentive for an experimental verification of the effect pointed out here.

Acknowledgment. This study was supported in part by a grant from the INDO-US subcommission. We are thankful to the anonymous referees for their critical comments on an earlier version of the manuscript.

References and Notes

(1) (a) Myers, A. B. *Chem. Rev.* **1996**, *96*, 911; (b) *Acc. Chem. Res.* **1997**, *30*, 519; (c) *J. Raman Spectrosc.* **1998**, *74*, 328.

- (2) Biswas, N.; Umapathy, S. *Curr. Sci.* **1998**, *74*, 328.
(3) Reber, C.; Zink, J. I. *J. Phys. Chem.* **1992**, *96*, 571.
(4) (a) Biswas, N.; Umapathy, S. *Pramana* **1997**, *48*, 937; (b) *J. Chem. Phys.* **1997**, *107*, 7849.
(5) Chakrabarti, N.; Kalyanaraman, C.; Sathyamurthy, N. *Chem. Phys. Lett.* **1997**, *267*, 31.
(6) (a) Biswas, N.; Umapathy, S.; Kalyanaraman, C.; Sathyamurthy, N. *Proc. Indian Acad. Sci. (Chem. Sci.)* **1995**, *107*, 233. (b) Balakrishnan, N.; Kalyanaraman, C.; Sathyamurthy, N. *Phys. Rep.* **1997**, *280*, 79.
(7) Levy, I.; Shapiro, M. *J. Chem. Phys.* **1988**, *89*, 2900.
(8) (a) Heller, E. J. *Acc. Chem. Res.* **1981**, *14*, 368. (b) Heller, E. J. *Potential Energy Surface and Dynamics Calculations*; Truhlar, D. G., Ed.; Plenum: New York, 1981.
(9) Kulander, K. C.; Heller, E. J. *J. Chem. Phys.* **1978**, *68*, 2439.
(10) Henriksen, N. E. *Adv. Chem. Phys.* **1995**, *XCI*, 433.
(11) Das, S.; Tannor, D. J. *J. Chem. Phys.* **1989**, *91*, 2324.
(12) Lee, S.-Y.; Heller, E. J. *J. Chem. Phys.* **1979**, *71*, 4777.
(13) Heller, E. J.; Sundberg, R. L.; Tannor, D. J. *J. Phys. Chem.* **1982**, *86*, 1822.